

A Miniature High Strain Rate Device

F. Akbaridoust, J. Philip and I. Marusic

Department of Mechanical Engineering
University of Melbourne, Victoria 3010, Australia

Abstract

Presented here are micro-PIV measurements of velocity and strain rate in a cross-slot region of a micro-cross channel. A micro-cross channel produces a homogeneous two-dimensional extensional flow with hyperbolic streamlines similar to Taylor's four-roll mill at larger scale. Due to the existence of the moving elements in four-roll mills, manufacturing a micron-sized four-roll mill is extremely challenging and consequently their applications are limited to the study of millimetre-scaled objects. Moreover, the natural instability of the flow in four-roll mills, caused by growing vortices at high rotational speed, limits the study of objects at high strain rates. Thanks to advances in micro-fluidics, the micro-cross channel is an alternative device for the four-roll mill without its restrictions. However, no systematic study has been carried out to measure the strain rate of the flow field in these devices. Apart from presenting a detailed procedure for the construction of micro-cross-channels, our micro-PIV results illustrate that high strain rates up to 24 s^{-1} can be reached, whereas 6 s^{-1} was the highest reported strain rate in a four-roll mill to date.

Introduction

Straining flow fields have been widely used to study the breakup and deformation of millimetre-sized droplets. Here hyperbolic or extensional flow is defined with streamlines $u = \gamma x$ and $v = -\gamma y$, where γ is the rate of strain. G. I. Taylor [13] first introduced the four-roll mill as a means of producing a pure extensional flow with hyperbolic streamlines in 1934. A wide range of studies have been carried out to measure the flow field in four-roll mills and also the break up of droplets in these devices [13, 15, 10]. Bentley and Leal [3] manufactured a computer controlled four-roll mill to confine the millimetre-sized particles and droplets and study the dynamics of them in an extensional flow with the strain rate of up to 5 s^{-1} . Anderotti et al. [1] later studied the intrinsic instability of the straining flow in a four-roll mill, from where they concluded the existence of counter rotating vortices that are aligned to the straining direction, which makes this flow unstable. They also experimentally demonstrated the negative feedback from rollers rotation on the strain rate at high rotational speed. They reached a maximum strain rate of 6 s^{-1} while the flow was still laminar with hyperbolic streamlines.

Although four-roll mills facilitate the study of the millimetre-sized object in the straining flow, due to the existence of the moving elements in four-roll mills, manufacturing micron-sized four-roll mills is most challenging. Also, producing a laminar stretching flow with hyperbolic streamlines at high rotational speed and high strain rates is limited. These restrictions stem from the growing vortices from the top and bottom of a four-roll mill that make the extensional flow intrinsically unstable [1]. Moreover, due to the low critical Reynolds number in four-roll mills, it is necessary to use highly viscous fluid such as glycerol or mixture of glycerol and water [13, 1]. These facts limit the usage of four-roll mill in studying the dynamics of micron-sized objects such as waterborne-microorganisms in hyperbolic flows.

The problem which motivated our study was a cyanobacterium, *Anaebena Circinalis* ($10 - 100 \mu\text{m}$ filaments), which is the cause of significant water contamination issues worldwide. Specifically, we are interested in the mechanical damage to cyanobacteria under the action of straining flow. The previous investigations of these species were carried out in turbulent flows [4, 14], from which anecdotal evidence of suspected mechanical damage was reported. Hence, our strategy here is to apply a spatially uniform high strain rate in a micro-cross channel to quantify the physical strength of these species. It should be noted that the highest achievable strain in four roll mills is below the range of the strain rate that allegedly leads to mechanical damage to the cyanobacteria filaments. In this paper, however, we focus only on the design and velocity characterisation of a miniature device to produce high straining flow.

Over the last two decades, the advances in microfluidics have opened up new vistas of studying micro-scale objects in fluid flows. A micro-cross channel is a device that is able to produce pure extensional flow similar to the four-roll mill at larger scale without the limitation of the four-roll mill. A micro-cross channel consists of two inlet channels with two converging laminar streams and two outlet channels with two diverging laminar streams. Both outlet channels set out perpendicularly to the inlet channels in a horizontal plane (see figure 1). In the cross-junction, where the two laminar flows interact each other, a two-dimensional straining flow with a zero-velocity (stagnation) point in the centre of the junction is generated. This flow contains a compressional axis along inlets and a extensional axis along outlets and has the same linear velocity equation in four-roll mill.

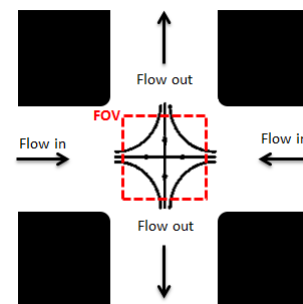


Figure 1: Schematic of a cross-slot junction

Largely the research in hyperbolic flows in micro-cross channels are divided into two categories. (1) The micro-channels are broadly used to investigate the instability of non-Newtonian fluids such as polymer solutions [2, 8]. (2) Thanks to the small dimensions of the micro-channels and existence of low Reynolds number even at high flow rates, it is used to study the dynamics of single cells, DNA molecules, micron-sized particles and droplets in the laminar straining water flows [11, 6, 12, 5].

Arratia et al. [2] studied the instability of extensional flow in a micro-cross channels, where they only observed the unstable

flow while using a non-Newtonian polymer solution, and they reported a stable hyperbolic flow while using a Newtonian fluid within the range of their Reynolds number. Rocha et al. [8] in numerically studied visco-elastic fluids and showed that rounding the corners marginally effected the instability of the flow.

Tanyeri et al. [11] developed a hydrodynamics trap to manipulate a micron-sized target object such as a DNA molecule and a fluorescent particle. Their device consisted of a micro-cross channel equipped with an on-chip membrane valve and a real-time feedback control to trap the target in the straining flow. The same group [12] also have parametrically studied the effect of parameters of the soft-lithography on the performance of the same trapping device. Later, Johnson-Chavarria et al. [5] improved their trap using two on-chip valves and applying an adaptive control algorithm for long-term manipulation of micron-sized target objects. However, no experimental measurements have been conducted to measure the velocity field and quantify the strain rate in the flow in these devices.

In the present work, a design of micro-cross channel similar to that was designed by Tanyeri et al. [11, 6, 12, 5] was used to measure the velocity field and the resulting strain rate in the flow using micro-PIV. The measured strain rate was compared to the maximum strain rate of the previous work in four-roll mill. Furthermore, we also report the uniformity of the strain rate over the cross-slot junction and the degree of fluctuation of the stagnation point was calculated.

Experimental Procedure

The schematic of the present micro-channel following Tanyeri et al. [11] is shown in figure 2. The target injection port was blocked as the flow measurement was done in the absence of any target object (e.g. cyanobacteria). The width and height of the cross-slot junction are $w = 400 \mu\text{m}$ and $h = 40 \mu\text{m}$, respectively. The single-layer micro-cross channel was fabricated using standard soft-lithography and micro-PIV was used to measure the velocity field and strain rate of water flow in the channel.

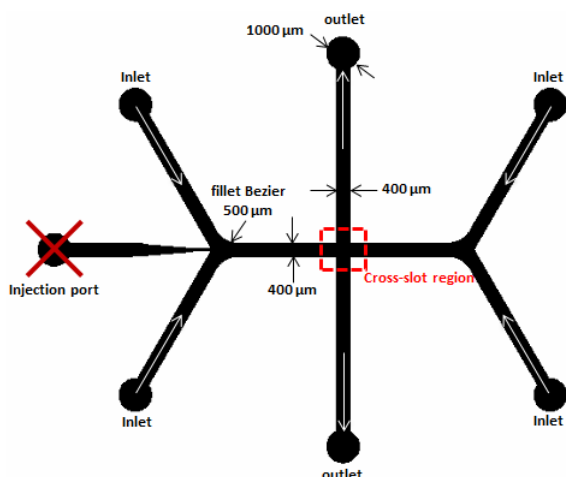


Figure 2: present micro-cross channel

Mould Fabrication

The features of the micro-channels shown in figure 2 was drawn two-dimensionally using Layout-Editor software and they were printed on a 5 in glass squared photo-mask.

A master mould was fabricated in a class 100 cleanroom in a yellow light environment. In order to make a master mould, a

puddle of negative epoxy-resist (SU-8 3050, MicroChem) was placed on a 4 in de-moisturised and clean silicon wafer. They were soft-baked on a clean hotplate at 65°C and 95°C for 3 and 6 min, respectively. Afterwards, the wafer and the SU-8 on top were spin-coated at 4000 rpm for 30 s to reach a $40 \mu\text{m}$ thick SU-8 layer [12]. To link the SU-8 to the silicon wafer, the silicon wafer with the spin-coated SU-8 and the photo-mask on top were exposed to UV light with an intensity of $150 \text{ mJ}/\text{cm}^2$. To finalise polymerisation they were post-baked at 65°C and 95°C for 1 and 6 min, respectively. To remove the uncured SU-8, the wafer was soaked in the SU-8 developer and then rinsed with SU-8 developer (Propylene glycol methyl ether acetate, MicroChem) and Isopropanol (IPA) until the features of the micro-channel appeared. The thickness of the micro-channel structures where measured under a profilometer with a resolution of 1 nm (Ambios XP200 Profiler).

PDMS Casting

Prior to polydimethylsiloxane (PDMS) casting, silanisation is required to help peel the PDMS off the mould by making the silicon substrate hydrophobic. To silanise the substrate, the wafer and $20 \mu\text{L}$ of silaniser (trichlorosilane) were placed in a desiccator under vacuum for 24 hours. To cast the PDMS on the mould, PDMS (Sylgard 184, Dow Corning) and its curing agent (Dow Corning) were mixed in a ratio of 1:10. Afterwards, the mixture was poured onto the mould to a thickness of approximately 5 mm. Then they were placed into a degassing desiccator for 30 min to remove all the bubbles. The mould and the liquid PDMS were baked in an oven at 65°C overnight. Thereafter, the PDMS replica was stripped off the mould. To establish connections between the micro-channel and the outside, all the access ports except the injection port were hole-punched using a blunt syringe needle (21 needle gauge, Zephyrtronics). In order to seal the micro-channel, the PDMS replica and a glass slide (1 mm thick, Waldemar Knittel) that was previously cleaned with IPA and dried with pressurised nitrogen were placed into a plasma cleaner (Harrick Plasma). Both surfaces of the glass slide and PDMS slab were treated by oxygen plasma under 300 mTorr for 2 min. Upon plasma cleaning, to reach an irreversible bond between PDMS slab and glass, PDMS replica were placed on the glass slide and pressed gently by hand. Finally, the device was baked again overnight to increase the bonding strength.

Micro-PIV Experimental Setup

In order to drive the fluid (distilled water containing seeding particles) into the micro-channel a gas-tight glass syringe ($1000 \mu\text{L}$ Hamilton) and a programmable syringe pump (Harvard PHD ULTRA) were used. A Luer lock adaptor and 24 gauge metal tubings were used to connect the PFA tubes to the syringe and the access ports of the microfluidic device via per-fluoroalkoxy (PFA) tubes ($0.020''$ inner diameter, $1/16''$ outer diameter, IDEX), respectively. To remove all the bubbles from the tubes and the micro channels, they were pre-filled with water and the pump delivered the fluid at $5000 \mu\text{L}/\text{hr}$ for 2 min to ensure that all the bubbles were removed. Then the flow rate was gradually decreased to $Q_{\text{total}} = 500 \mu\text{L}/\text{hr}$.

As shown in figure 3, the micro-channel was mounted on an inverted TI-U eclipse Nikon microscope with a CFI S Plan Fluor ELWD 20X (NA = 0.45) objective. The microscope was coupled with a 532 nm Nd-YAG double-pulsed laser (EverGreen) to illuminate the $1 \mu\text{m}$ red fluorescent particles (ThermoFisher) that absorb green light and emit red light. To separate the wavelengths a G-2A Nikon cube filter that includes dichroic mirror, barrier and excitation filter was used. Consequently, the camera sensor only acquires the light emitted by the particles, thereby reducing background noise in the image field. A high speed

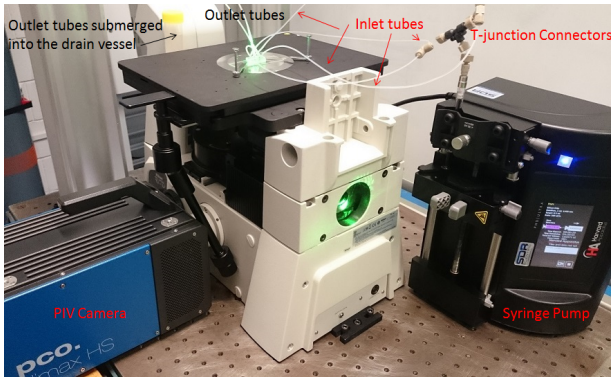


Figure 3: Experimental Setup

CCD sensor camera (2000×2000 , 12 bits, PCO.dimax HS4) was used to capture the particle images. Figure 4 shows an inverted and overlaid of six pairs of particles images with $\Delta t = 2$ ms from the cross-slot junction.

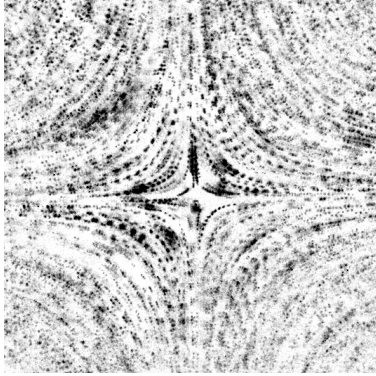


Figure 4: Inverted and overlaid six pairs of particles images with $\Delta t = 2$ ms

In micro-PIV the depth of field is equal to the depth of focus of the microscope objective, which is $5.6 \mu\text{m}$ in the present experiment. A multi-grid algorithm with the initial interrogation window size of 64×64 pixels and final size of 32×32 with 50% overlap were applied to correlate the images.

Results and Discussions

The velocity vector map, smoothed by a 3×3 median filter, in a $350 \mu\text{m} \times 350 \mu\text{m}$ central region of the cross-slot junction (figure 1) at the flow rate of $500 \mu\text{L/hr}$ is shown in figure 5. To calculate the strain rate, a Savitzky-Golay differentiation filter was fitted to a set of 5×5 velocity data points to a third-order polynomial in the least-squares sense. The spatially averaged strain rate over a $200 \mu\text{m} \times 200 \mu\text{m}$ ($w/2 \times w/2$) central region of the cross-slot junction is $\gamma = 24.61 \text{ s}^{-1}$. The strain rate is reasonably constant over the this region with the relative standard deviation of 2%.

In order to compare the measured velocity field and the uniformity of the strain rate to an ideal hyperbolic flow, equations $u = \gamma_{eq}(x - x_0)$; $v = -\gamma_{eq}(y - y_0)$ that present a pure hyperbolic velocity field with a centre of x_0 and y_0 were fitted to the velocity field (figure 5) with a least-square approximation. Where γ_{eq} , x_0 and y_0 are the unknown parameters, and the number of the equations are equal to twice the number of velocity vectors per image. In the other words, for each velocity vector, two equations are available. By using the strain rate that was obtained from each data point, these equations could be converted

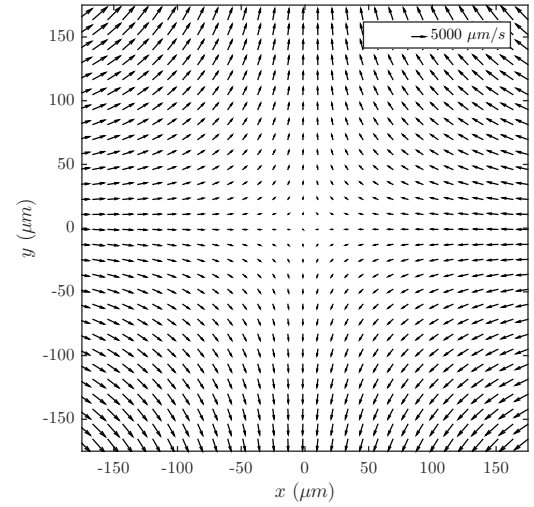


Figure 5: Vector map of the FOV in the cross slot-junction at $500 \mu\text{L/hr}$

to linear equations. Therefore, linear equations were solved, and x_0 and y_0 were obtained in the least-squares sense. However, in order to obtain more accurate results, the obtained x_0 and y_0 were used as initial conditions to solve the non-linear equations. Subsequently, non-linear equations were solved using a Newton-Raphson method and the position of centre and the equivalent strain rate were obtained. The equivalent strain rate of the fitted pure hyperbolic flow equation is $\gamma_{eq} = 24.56 \text{ s}^{-1}$. This value well agreed with the spatially averaged strain rate $\gamma = 24.61 \text{ s}^{-1}$. Figure 6 shows the least square fit of u and v and the error bars are twice the standard deviation for a 95% confidence level for u and v .

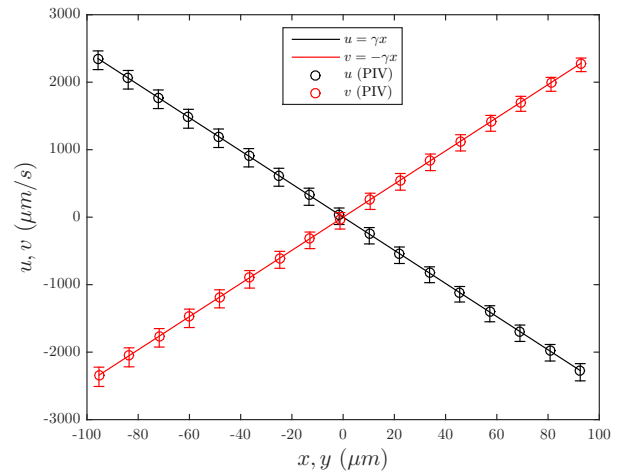


Figure 6: Distributions of velocity components and errors in the micro-channel

Figure 7 shows the centre variation with time. The standard deviation of the centre variation in x and y -directions are $0.50 \mu\text{m}$ and $0.63 \mu\text{m}$, respectively. This result confirms the possibility of the trapping and confining a target object larger than $1 \mu\text{m}$ at the zero-velocity point at $500 \mu\text{L/hr}$.

By comparing the obtained strain rate to those of previous studies in a four-roll mill, it is shown that strain rates of up to 24 s^{-1}

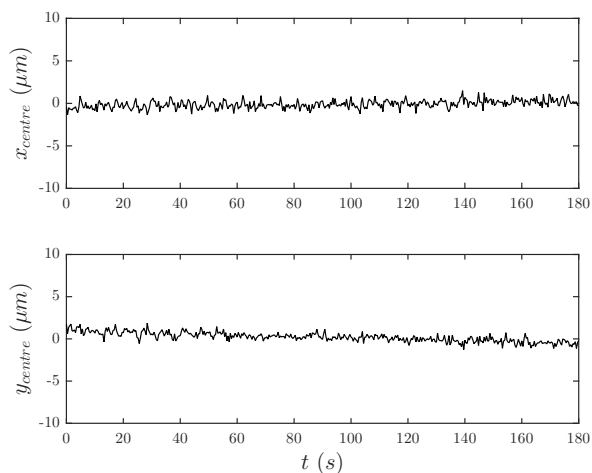


Figure 7: Fluctuation of the stagnation point in the x and y -direction

could be reached in this microfluidic device, whereas 6 s^{-1} was the highest reported strain rate in four-roll mills [1]. Therefore, not only does a microcross-channel enable the study of micron-sized objects in a uniform straining flow, but it also provides the possibility of applying a high strain rate to micron-scaled object.

In the previous work carried out by Tanyeri et al., the flow rates were between $20 \text{ }\mu\text{L/hr}$ and $100 \text{ }\mu\text{L/hr}$, this range of flow rate generates strain rates between 1 and 4 s^{-1} , based on an approximate formula $\gamma = Q_{total}/(hw^2)$ for calculation of the strain rate in this flow, rather than direct measurements [7]. This range of strain rate was enough to stretch a DNA molecule [9]. However, to stretch or break a waterborne-microorganism such as cyanobacteria, a high strain rate range of 10 and 18 s^{-1} is required [14]. The strain rate achieved in this study confirms the possibility of studying cyanobacteria in a spatially uniform strain rate flow.

Conclusions

Studying the dynamics of the micron-sized objects in a laminar extensional flow with high strain rates has always been challenging by employing the four-roll mill, which is the most common means of producing this type of flow. The limitation of reaching high strain rates is rooted in the natural instability of the flow in the four-roll mill due to the growing vortices from the bottom and top walls of the apparatus at high rotational speed. Also, manufacturing a micron-sized four-roll mill is a restriction of studying the dynamics of micron-scale target objects in this device. Here we fabricated and quantified the flow in a micro-cross channel that was previously used to manipulate and confine micron-sized objects without the characterisation of the flow field. We measured the velocity field and calculated the strain rate in this micro-channel using micro-PIV. The strain rate obtained in the cross-slot junction was four times higher than that of the four-roll mill using water. We also calculated the variation of the strain rate and fluctuation of the stagnation point position, which was found to be minimal leading us to ascertain the suitability of testing cyanobacteria.

Acknowledgements

The authors gratefully acknowledge Australian Research Council for the financial support of this work.

This work was performed in part at the Melbourne Centre for

Nanofabrication (MCN) in the Victorian Node of the Australian National Fabrication Facility (ANFF).

References

- [1] Andreotti, B., Douady, S. and Couder, Y., An experiment on two aspects of the interaction between strain and vorticity, *Journal of Fluid Mechanics*, **444**, 2001, 151–174.
- [2] Arratia, P. E., Thomas, C., Diorio, J. and Gollub, J. P., Elastic instabilities of polymer solutions in cross-channel flow, *Physical Review Letters*, **96**, 2006, 144502.
- [3] Bentley, B. and Leal, L., Computer-controlled four-roll mill for investigations of particle and drop dynamics in two-dimensional linear shear flows, *Journal of Fluid Mechanics*, **167**, 1986, 219–40.
- [4] Hondzo, M. and Wuest, A., Do microscopic organisms feel turbulent flows?, *Environmental science & technology*, **43**, 2008, 764–768.
- [5] Johnson-Chavarria, E. M., Agrawal, U., Tanyeri, M., Kuhlman, T. E. and Schroeder, C. M., Automated single cell microreactor for monitoring intracellular dynamics and cell growth in free solution, *Lab on a Chip*, **14**, 2014, 2688–2697.
- [6] Johnson-Chavarria, E. M., Tanyeri, M. and Schroeder, C. M., A microfluidic-based hydrodynamic trap for single particles, *JoVE (Journal of Visualized Experiments)*, e2517–e2517.
- [7] Mulligan, M. K. and Rothstein, J. P., The effect of confinement-induced shear on drop deformation and breakup in microfluidic extensional flows, *Physics of Fluids (1994-present)*, **23**, 2011, 022004.
- [8] Rocha, G. N., Poole, R. J., Alves, M. A. and Oliveira, P. J., On extensibility effects in the cross-slot flow bifurcation, *Journal of Non-Newtonian Fluid Mechanics*, **156**, 2009, 58–69.
- [9] Schroeder, C. M., Babcock, H. P., Shaqfeh, E. S. and Chu, S., Observation of polymer conformation hysteresis in extensional flow, *Science*, **301**, 2003, 1515–1519.
- [10] Stone, H., Bentley, B. and Leal, L., Experimental study of transient effects in the breakup of viscous drops, *Journal of Fluid Mechanics*, **173**, 1986, 131.
- [11] Tanyeri, M., Johnson-Chavarria, E. M. and Schroeder, C. M., Hydrodynamic trap for single particles and cells, *Applied Physics Letters*, **96**, 2010, 224101.
- [12] Tanyeri, M., Ranka, M., Sittipolkul, N. and Schroeder, C. M., Microfluidic wheatstone bridge for rapid sample analysis, *Lab on a Chip*, **11**, 2011, 4181–4186.
- [13] Taylor, G., The formation of emulsions in definable fields of flow, *Proceedings of the Royal Society of London. Series A, Containing Papers of a Mathematical and Physical Character*, **146**, 1934, 501–523.
- [14] Thomas, W. H. and Gibson, C. H., Effects of small-scale turbulence on microalgae, *Journal of Applied Phycology*, **2**, 1990, 71–77.
- [15] Wang, J., Han, J. and Yu, D., Numerical studies of geometry effects of a two-dimensional microfluidic four-roll mill on droplet elongation and rotation, *Engineering Analysis with Boundary Elements*, **36**, 2012, 1453–1464.